ISBN: 978-3-95450-231-8 ISSN: 2673-5490 doi: 10.18429/JACoW-IPAC2023-TUPL014

SENSITIVITY OF THE OPTICAL-KLYSTRON-BASED HIGH-GAIN HARMONIC GENERATION ON THE ELECTRON BEAM ENERGY PROFILE

G. Paraskaki*, E. Ferrari, L. Schaper, E. Schneidmiller, DESY, Germany
E. Allaria, Elettra-Sincrotrone Trieste S.C.p.A., Trieste, Italy

Abstract

Externally seeded free electron lasers (FELs) offer fully coherent and stable FEL radiation in the soft x-ray regime. While electron bunches of superconducting-based FELs are available at MHz repetition rates, seeded radiation is limited by the repetition rate of the seed laser used in the process. Combining standard seeding schemes with an optical klystron is a simple and promising trick to reduce the seed laser power requirements and allow externally seeded radiation at higher repetition rates. To ensure optimum operation, we study the combined effect of a linear and a quadratic electron beam energy chirp on the properties of the output FEL radiation.

INTRODUCTION

High-gain FELs all around the world have been making enormous progress during recent years which is driven by the wishes of users for special FEL pulse properties required by their experiments [1]. While self-amplified spontaneous emission [2, 3] has been the base for experiments in high-gain FELs for over a decade, different techniques have been proposed and tested to overcome the limitations of SASE, namely the poor longitudinal coherence and the low shot-to-shot stability. For this purpose, external seeding techniques [4, 5] have become a popular and reliable alternative among the FEL community [6, 7]. In this type of FEL operation, an external seed laser is used to initiate the FEL process and to transfer its unique properties to those of the output FEL radiation. In the case where external seeding is combined with the harmonic generation, the output FEL wavelength is a harmonic of the seed laser wavelength. While the properties of the seeded output FEL are excellent in coherence and stability, the highest repetition rate and the shortest possible wavelength are in most cases limited by the seed laser.

The shortest possible output FEL wavelength of an externally seeded FEL is determined by the seed laser wavelength and the harmonic conversion that can be achieved. The highest repetition rate is determined by the repetition rate of the seeded laser, assuming that high repetition rate electron bunches are available with the superconducting-based FEL linear accelerators (linacs) [8–11]. Seed lasers suitable for seeded operation are in turn limited in the shortest wavelength and highest repetition rate available mainly due to the high peak power required for the process. For instance, high-gain harmonic generation (HGHG) [4] requires a seed laser with enough power to induce an electron beam energy modulation several times larger than the initial energy spread, which translates into several tens to hundreds of MW for typical seeding parameters. It is realistic to say that seed lasers with sufficient peak power for seeding are until now limited to the ultraviolet (UV) wavelength range and to the range of tens to hundreds of Hz. FLASH is already planning to extend this limit with multiple hundreds of pulses per second with its upcoming upgrade, FLASH2020+ [12].

To overcome this hurdle, a modified high-gain harmonic generation scheme, called optical-klystron-based high-gain harmonic generation, was proposed [13, 14]. The modifications in the setup aim at reducing the seed laser power requirements by two to three orders of magnitude [14] as it will be explained in detail in the following section. This significant reduction allows seed lasers to operate at a higher repetition rate, or at a shorter wavelength, extending in this way the shortest achievable wavelength and/or its highest repetition rate. While the first experimental results have already been published [13], the full potential of this promising scheme has not yet been fully explored. In preparation for upcoming experiments, here we take the opportunity to address the impact of the electron beam energy profile on the scheme. Typically, the energy profile of the electron beam varies for different machines and purposes. With this study, we want to explore the effect of non-ideal electron beams on the optical-klystron-based HGHG. In the past, we showed results for an isolated linear energy chirp [15] and an isolated quadratic electron beam energy chirp [16]. Here, we expand the study towards a more realistic case, where the two different order terms are combined.

Layout

In a standard HGHG scheme, a seed laser with a high peak power is required to modulate the electron beam energy in a short undulator called a modulator. This energy modulation can then be translated into a longitudinal density modulation with the assistance of a dispersive section such as a chicane, as shown in Fig 1. For a fixed modulator length, by tuning the peak power of the seed laser and the dispersive strength of the chicane it is possible to obtain bunching at a harmonic of the seed laser wavelength. The radiators are then tuned to be resonant at this wavelength and the result is that fully coherent radiation at the harmonic of the seed laser wavelength is generated.

* georgia.paraskaki@desy.de

ISBN: 978-3-95450-231-8 ISSN: 2673-5490 doi: 10.18429/JACoW-IPAC2023-TUPL014

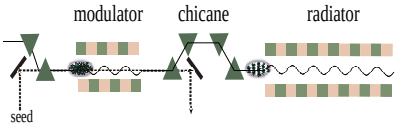

Figure 1: In the standard HGHG scheme, a high-power seed laser is preparing the electron bunches to generate fully coherent radiation at a harmonic of its wavelength.

In this standard HGHG scheme, in order to achieve a relatively high harmonic for the given scheme, on the order of h=15, it is necessary to use a seed laser of a high peak power that will allow us to modulate the energy of the electrons by a factor of roughly 10-15 with respect to the initial energy spread. While this is possible for low repetition rate UV seed lasers, this is impossible for shorter wavelength or higher repetition rate seed lasers. To allow a higher repetition rate, the peak power requirements of the seed laser must be reduced as follows: An additional chicane and modulator are incorporated in the new, optical-klystron-based HGHG which is shown in Fig. 2. This time, we use a lower-power seed laser in the first modulator, aiming at bunching at the fundamental wavelength after chicane 1, for which an energy modulation comparable to the energy spread is sufficient. Starting the modulation process on modulator 2 with bunching at the fundamental allows for self-amplification to amplitudes that are suitable for generating bunching at high harmonics.

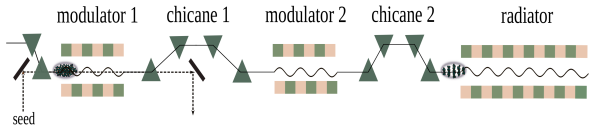

Figure 2: In the optical-klystron-based HGHG scheme, the layout is modified to allow reducing the power required by the seed laser, while still obtaining fully coherent radiation at harmonics of its wavelength.

As shown with simulations in detail in [14], this way it is possible to obtain with the optical-klystron-based HGHG similar output FEL pulses at the 15th harmonic of the seed laser wavelength and with roughly 360 times lower seed laser peak power.

Simulations

As a continuation of our previous studies, here we simulate the optical-klystron-based HGHG scheme incorporated into the FLASH2020+ lattice, thus the beamline that will be built for the upgrade of FLASH1 beamline at DESY [12]. A summary of the simulation parameters can be found in Table 1. All simulations presented here are implemented with the code Genesis 1.3 v4 [17].

In order to study the combined effect of the linear and quadratic energy chirp, we look into 4 different cases for the energy profile of the electron beam, described here as a polynomial $\gamma = \gamma_0 + c_1 s + c_2 s^2$:

1. **Case A:** no linear chirp, no quadratic chirp.

Table 1: Input Simulation Parameters

Electron beam	
Energy	750 MeV
Uncorrelated energy spread	75 keV
Peak current	500 A (flat-top)
Seed laser	
Wavelength	300 nm
rms duration	33 fs (rms)

2. **Case B:** no linear chirp, quadratic chirp $c_2 = 50 \cdot 10^7 \mathrm{m}^{-2}$.
3. **Case C:** linear chirp $c_1 = -7.4 \cdot 10^4 \mathrm{m}^{-1}$, no quadratic chirp.
4. **Case D:** linear chirp $c_1 = -7.4 \cdot 10^4 \mathrm{m}^{-1}$, quadratic chirp $c_2 = 50 \cdot 10^7 \mathrm{m}^{-2}$.

The linear chirp of $c_1 = -7.4 \cdot 10^4 \mathrm{m}^{-1}$ is equivalent to a relative energy chirp of $h = 50\ \mathrm{m}^{-1}$, defined as $h = \frac{dE}{ds}\frac{1}{E}$. In all cases, the central energy is $\gamma_0 = 1467.7$ and the temporal position of this reference energy overlaps with the center of the current profile. The seed laser peak power is placed in all cases at a temporal position −15 fs with respect to the central energy to account for the slippage along the two modulators. The energy profiles for the 4 cases we study are shown in Fig. 3 with respect to the position of the seed laser and the current profile. The duration of the current profile is kept short to allow for faster simulations.

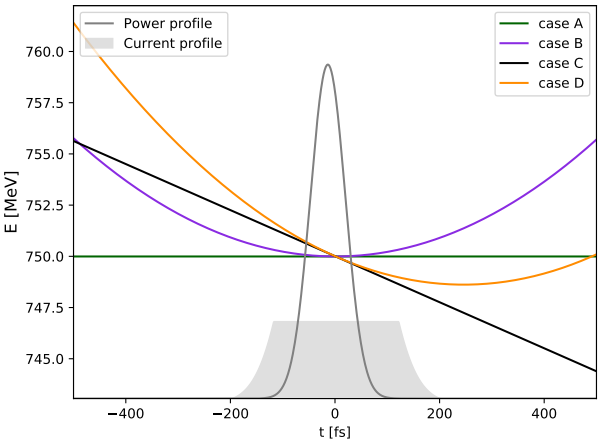

Figure 3: Initial conditions in simulations. The current and seed laser power profile remain the same for all simulations. The energy profile changes while keeping the reference energy at the same temporal position t=0 fs. The temporal position of the current profile and the seed laser power profile are illustrated for reference.

In all 4 cases, we aim at the 15th harmonic of a 300 nm seed laser wavelength and at a final wavelength of 20 nm. The bunching at the entrance of the radiators is roughly

ISBN: 978-3-95450-231-8 ISSN: 2673-5490 doi: 10.18429/JACoW-IPAC2023-TUPL014

7% in all cases and the optimization of the modulator and radiator parameters K is done in each case individually. We show the output FEL in time and frequency domain for all cases in Fig. 4a and Fig. 4b, respectively. The pulse energy growth along the radiators is shown in Fig. 4c. The most important properties to characterize the output FEL pulses are listed in Table 2.

Initially, we compare the cases with no quadratic chirp and we notice that apart from the well-predicted wavelength shift [15], the pulse properties are comparable and the output FEL performance remains the same. Adding the quadratic chirp in general leads to a broader bandwidth and a relatively shorter wavelength. It becomes clear that when adding the quadratic chirp the pulse duration is reduced due to the faster variation of the electron beam energy in time. The effect is more severe for case B, where we have only the quadratic term as shown in the pulse energy curve in Fig. 4c.

Table 2: Pulse Properties of the Output FEL Radiation shown in Fig. 4.

$c_1 = 0\ \mathrm{m}^{-1}$:	$c_2 = 0\ \mathrm{m}^{-2}$	$c_2 = 50 \cdot 10^7\ \mathrm{m}^{-2}$
Pulse energy	28.1 µJ	20.6 µJ
FWHM BW	$7.4 \cdot 10^{-4}$	$2.2 \cdot 10^{-3}$
rms duration	21.1 fs	18.5 fs
$c_1 = -7.4 \cdot 10^4\ \mathrm{m}^{-1}$:	$c_2 = 0\ \mathrm{m}^{-2}$	$c_2 = 50 \cdot 10^7\ \mathrm{m}^{-2}$
Pulse energy	28.9 µJ	23.2 µJ
FWHM BW	$7.1 \cdot 10^{-4}$	$6.4 \cdot 10^{-3}$
rms duration	24 fs	21.6 fs

Outlook

In this paper, we have studied the effect of the electron beam energy chirp on the optical-klystron-based HGHG scheme. More specifically, we have investigated the effect of the combined linear and quadratic terms. This study allows us to go closer to a start-to-end beam and a more realistic case. In our following studies, we are planning to explore more combinations of chirps, seed durations and different longitudinal positions of the seed laser, taking advantage of the possibility of fixing the seed laser temporal position in an experiment as we wish. This way, we will be able to determine optimized conditions for a given longitudinal phase space of a machine and to interpret any deviations measured with respect to the ideal case.

ACKNOWLEDGEMENTS

The authors would like to thank Pardis Niknejadi for her support in post-processing electron beam distributions generated by Genesis 1.3 v4. We acknowledge DESY, Germany, a member of the Helmholtz Association HGF, for the provision of experimental facilities. This work has been carried out at FLASH.

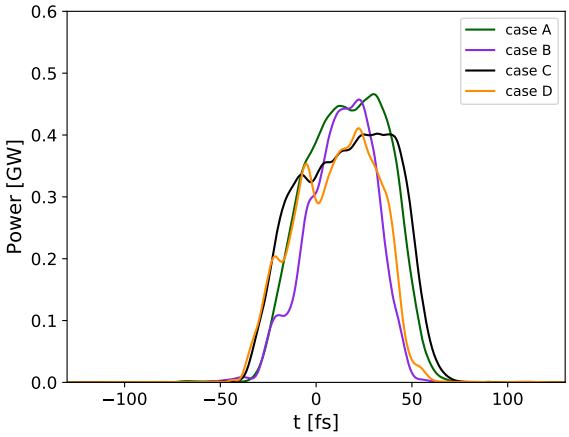

(a)

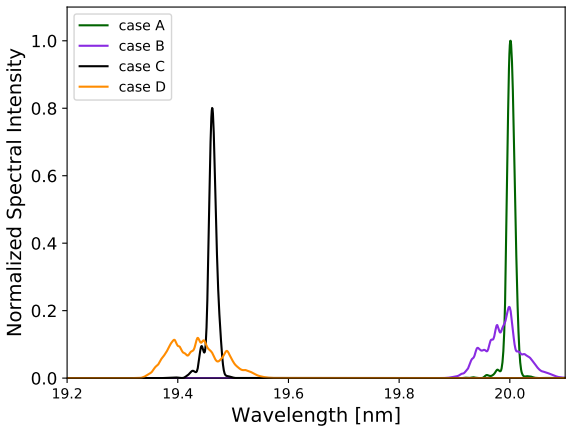

(b)

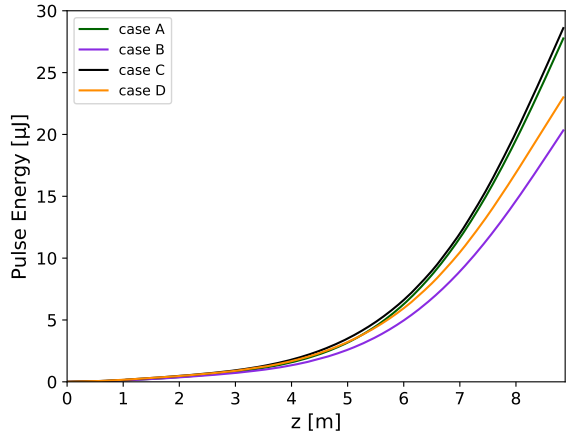

(c)

Figure 4: Output FEL radiation from the optical-klystron HGHG scheme: (a) Power profile, (b) spectra and (c) growth of the pulse energy along the radiator for the three different electron beam energy profiles shown in Fig. 3.

ISBN: 978-3-95450-231-8 ISSN: 2673-5490 doi: 10.18429/JACoW-IPAC2023-TUPL014

REFERENCES

[1] P. R. Ribic and G. Margaritondo, "Status and prospects of x-ray free-electron lasers (x-FELs): a simple presentation," *J. Phys. D: Appl. Phys.*, vol. 45, p. 213001, 2012. doi:10.1088/0022-3727/45/21/213001

[2] A. M. Kondratenko and E.L. Saldin, "Generation of coherent radiation by a relativistic electron beam in an ondulator", *Part. Accel.*, vol. 10, pp. 207–216, 1980.

[3] R. Bonifacio, F. Casagrande and G. Casati. "Cooperative and chaotic transition of a free electron laser Hamiltonian model", *Opt. Comm.*, vol. 40, pp. 219-223, 1982. doi:10.1016/0030-4018(82)90265-6

[4] L. H. Yu and J. Wu, "Theory of high gain harmonic generation: an analytical estimate", *Nucl. Instr. Meth.*, vol. 483, pp. 493-498, 2002. doi:10.1016/S0168-9002(02)00368-6

[5] G. Stupakov, "Using the Beam-Echo Effect for Generation of Short-Wavelength Radiation", *Phys. Rev. Lett.*, vol. 102, p. 074801, 2007. doi:10.1103/PhysRevLett.102.074801

[6] P. Ribic *et al.*, "Coherent soft X-ray pulses from an echo-enabled harmonic generation free-electron laser", *Nat. Photonics*, vol. 13, pp. 1–7, 2019. doi:10.1038/s41566-019-0427-1

[7] E. Allaria, R. Appio, L. Badano, *et al.*, "Highly coherent and stable pulses from the FERMI seeded free-electron laser in the extreme ultraviolet", *Nat. Photonics*, vol. 6, pp. 699–704, 2012. doi:10.1038/nphoton.2012.233

[8] J. Rossbach, J. R. Schneider, and W. Wurth "10 years of pioneering x-ray science at the free- electron laser flash at DESY", *Phys. Rep.*, vol. 808, pp. 1–74, 2019. doi:10.1016/j.physrep.2019.02.002

[9] D. Nölle, "FEL Operation at the European XFEL Facility", in *Proc. FEL'19*, Hamburg, Germany, Aug. 2019, pp. 766–771. doi:10.18429/JACoW-FEL2019-FRA01

[10] T. Liu, X. Dong, and C. Feng, "Start-to-end Simulations of the Reflection Hard X-Ray Self-Seeding at the SHINE Project", in *Proc. FEL'19*, Hamburg, Germany, Aug. 2019, pp. 254–257. doi:10.18429/JACoW-FEL2019-TUP087

[11] E. Hemsing *et al.*, "Soft x-ray seeding studies for the SLAC Linac Coherent Light Source II" , *Phys. Rev. Accel. Beams*, vol. 22, p. 110701, 2019. doi:10.1103PhysRevAccelBeams.22.110701

[12] L. Schaper *et al.*, "Flexible and Coherent Soft X-ray Pulses at High Repetition Rate: Current Research and Perspectives", *Appl. Sci.*, vol. 11, p. 9729, 2021. doi:10.3390/app11209729

[13] J. Yan *et al.*, "Self-amplification of Coherent Energy Modulation in Seeded Free-Electron Lasers", *Phys. Rev. Lett.*, vol. 126, p. 084801, 2021. doi:10.1103/PhysRevLett.126.084801

[14] G. Paraskaki, E. Allaria, E. Schneidmiller, and W. Hillert, "High repetition rate seeded free electron laser with an optical klystron in high-gain harmonic generation", *Phys. Rev. Accel. Beams*, vol. 24, p. 120701, 2021. doi:10.1103/PhysRevAccelBeams.24.120701

[15] G. Paraskaki, E. Allaria, E. Ferrari, W. Hillert, L. Schaper, and E. Schneidmiller, "Path to High Repetition Rate Seeding: Combining High Gain Harmonic Generation with an Optical Klystron", in *Proc. IPAC'22*, Bangkok, Thailand, Jun. 2022, pp. 2411–2414. doi:10.18429/JACoW-IPAC2022-THOXSP3

[16] G. Paraskaki, E. Ferrari, L. Schaper, E. Schneidmiller, and E. Allaria, "Impact of Electron Beam Energy Chirp on Optical-Klystron-Based High Gain Harmonic Generation", presented at the FEL2022, Triest, Italy, Aug. 2022, paper TUP49, to be published.

[17] S. Reiche, "Genesis 1.3: a fully 3d time-dependent fel simulation code", *Nucl. Instrum. Meth. Phys. Res. Sect. A*, vol. 429, pp. 243-248, 1999. doi:10.1016/S0168-9002(99)00114-X